



Controlled thermal decomposition of NaSi to derive silicon clathrate compounds

Hiro-omi Horie, Takashi Kikudome, Kyosuke Teramura, Shoji Yamanaka *

Department of Applied Chemistry, Graduate School of Engineering, Hiroshima University, Higashi-Hiroshima 739-8527, Japan

ARTICLE INFO

Article history:

Received 18 June 2008

Received in revised form

30 September 2008

Accepted 5 October 2008

Available online 18 October 2008

Keywords:

Silicon clathrate

Thermal decomposition

Sodium monosilicide

ABSTRACT

Formation conditions of two types of sodium containing silicon clathrate compounds were determined by the controlled thermal decomposition of sodium monosilicide NaSi under vacuum. The decomposition began at 360 °C. Much higher decomposition temperatures and the presence of sodium metal vapor were favorable for the formation of type I clathrate compound Na₈Si₄₆. Type II clathrate compound Na_xSi₁₃₆ was obtained as a single phase at a decomposition temperature <440 °C under the condition without sodium metal vapor. The type I clathrate compound was decomposed to crystalline Si above 520 °C. The type II clathrate compound was thermally more stable, and retained at least up to 550 °C in vacuum.

© 2008 Elsevier Inc. All rights reserved.

1. Introduction

The first silicon clathrate compounds isostructural with the two clathrate-type gas (G) hydrates (types I and II with the compositions of G_x(H₂O)₄₆ and G_x(H₂O)₁₃₆ in the unit cells, respectively) were obtained by Cros et al. [1–3] in the late 1960s by the thermal decomposition of the Zintl-phase NaSi. In the silicon clathrate compounds, the H–O···H hydrogen bonds of the gas hydrates are replaced with Si–Si covalent bonds, sodium atoms instead of gas (G) molecules of the hydrates being trapped in the cages formed by the Si–sp³ covalent network. The crystal structures of the two types of silicon clathrate compounds are schematically shown in Fig. 1. Type I silicon clathrate Na₈Si₄₆ is composed of face sharing silicon dodecahedra (@Si₂₀) and silicon tetrakaidecahedra (@Si₂₄); all of the polyhedral cages are occupied by Na atoms. Type II silicon clathrate Na_xSi₁₃₆ (x ≤ 24) has a more open framework, and is composed of face sharing silicon dodecahedra (@Si₂₀) and silicon hexakaidecahedra (@Si₂₈). In the type II Si clathrate, the occupancy of the polyhedral cages by Na atoms varies depending on the preparation conditions [4,5]. Very recently, a silicon-based type III clathrate compound Si_{172–x}P_xTe_y has been prepared [6], which is isomorphous with the type III gas hydrate [(Br₂)₂₀□₁₀](H₂O)₁₇₂, and tin clathrates Cs₃₀Na_{1.33x–10}Sn_{172–x} and Cs_{13.8}Rb_{16.2}Na_{1.33x–10}Sn_{172–x} [7]. Recent reviews on group 14 (Si, Ge, and Sn) clathrates have been given by Bobev and Sevov [8], Beekman and Nolas [9], San-Miguel and Toulmonde [10], and Konvnr and Shevelkov [11].

So far a number of clathrate-type compounds made of group 14 elements in the frameworks have been prepared; the isomorphous substitution of the framework atoms coupled with alkali, alkaline-earth and rare-earth metals placed in the cages have produced more than 110 phases mainly with the type I clathrate structure [8,12]. Recently much attention has been revived on their physical properties based on the unique open framework structures, such as thermoelectric properties and superconductivity [9,13,14]. Electroconductive clathrate compounds with metal atoms rattling in the cages are expected to be promising thermoelectric materials owing to their low thermal conductivities [13]. The low thermal conductivities of Sr₈Ga₁₆Ge₃₀ [15,16] and Ba₈Ga₁₆Sn₃₀ [17] have been well characterized and interpreted in terms of the rattling of the heavy metal atoms in the cages. Barium containing silicon clathrate compounds, Ba₆Na₂Si₄₆ [18] and Ba₈Si₄₆ [19], became the first superconductors with Si–sp³ covalent frameworks. The Si clathrate compound without metal guest atoms can be a new Si allotrope [20–22], which has a wide band gap compared with diamond structured Si. The new Ge allotrope Ge₁₃₆ with the guest-free type II clathrate structure was prepared by the oxidation of a precursor with the nominal composition NaGe_{2.25} [23]. Ab initio calculation by Moruguchi et al. [24] suggested that some type II clathrate alloys Si_{136–x}Ge_x could be direct band gap semiconductors, and expected to have interesting optoelectronic as well as photovoltaic applications [9].

Clathrate compounds with substituted frameworks are classified into Zintl compounds. For instance, Sr₈Ga₁₆Ge₃₀ has a formal charge (Sr²⁺)₈[(Ga^{–1})₁₆(Ge⁰)₃₀]^{16–} so that all of the framework atoms can have octet configurations to complete the sp³ four-fold covalent bonds. The compositions are electrically balanced as an

* Corresponding author. Fax: +81 82 424 7740.

E-mail address: syamana@hiroshima-u.ac.jp (S. Yamanaka).

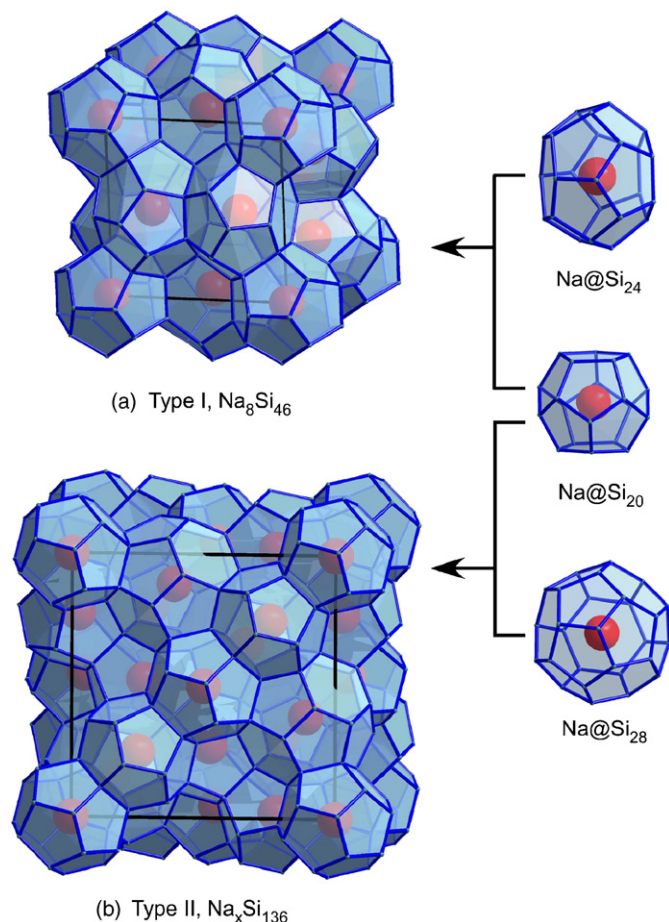


Fig. 1. Schematic structural models of clathrate compounds: (a) type I $\text{Na}_8\text{Si}_{46}$ and (b) type II $\text{Na}_x\text{Si}_{136}$.

ionic compound. Most of Zintl type clathrate compounds are prepared by a simple direct melting of the stoichiometric mixtures of the constituent elements at high temperatures. A slight deviation from the stoichiometric composition can produce n- or p-type clathrate compounds, which are interesting candidates for thermoelectric applications. Clathrate compounds without framework substitution can be characterized as intercalation compounds [25], since the framework atoms fulfill the octet configurations without the aid of the electrons from the guest metal atoms in the cages. The metal atoms are intercalated in the cages. Most of the intercalation type clathrate compounds cannot be prepared by a simple melting. $\text{Na}_8\text{Si}_{46}$ and $\text{Na}_x\text{Si}_{136}$ were prepared by the thermal decomposition of the Zintl phase NaSi. Barium containing superconductor $\text{Na}_2\text{B}_6\text{Si}_{46}$ was also prepared by decomposition of the Zintl phase Na_2BaSi_4 [26]. $\text{Ba}_8\text{Si}_{46}$ is prepared only under a high pressure and high temperature condition from the mixture of 8 BaSi_2+30 Si [19]. The metal fully occupied type II clathrates $\text{A}_8\text{Na}_{16}\text{E}_{136}$ ($A = \text{Rb}, \text{Cs}$; $E = \text{Si}, \text{Ge}$) have been prepared by a direct reaction of the element mixtures. The driving force of the formation can be ascribed to the distinguished difference of the atomic sizes between A and Na; A atoms occupy the hexakaidecahedral cages, and Na atoms the smaller dodecahedral cages. The smaller Na ions can be deintercalated by evacuation at elevated temperatures leaving $\text{Cs}_8\text{Ge}_{136}$ [27].

It is interesting to note that the first Si clathrate found by Cros et al. [1–3] is the most difficult clathrate to prepare. Type I Si clathrate $\text{Na}_8\text{Si}_{46}$ was prepared by removing a part of Na atoms from NaSi under Ar atmosphere at 410 °C [14,20]. Type II Si clathrates $\text{Na}_x\text{Si}_{136}$ were prepared in a similar way by removing Na

atoms at temperatures ranging 350–440 °C, but under vacuum [4,5]. Most of the type II Si clathrate samples so far obtained were mixtures containing the type I phase. Ramachandran et al. [5] separated the two phases by using heavy liquid floatation.

Recently much attention has been attracted to the synthesis of the type II Si clathrate compound, since the type II clathrate compound can have tunable compositions $\text{Na}_x\text{Si}_{136}$ ($0 \leq x \leq 24$) [8], and accordingly the transport properties can be tuned by the Na content. In order to achieve the detailed characterization of the type II Si clathrate compounds, the synthesis of the type II clathrate compound with a desired composition without contamination of the type I clathrate compound has been strongly desired. The formation conditions and mechanisms should be clarified. In this paper, the formation regions of the two types of clathrates have been studied by using controlled decomposition of NaSi.

2. Experimental

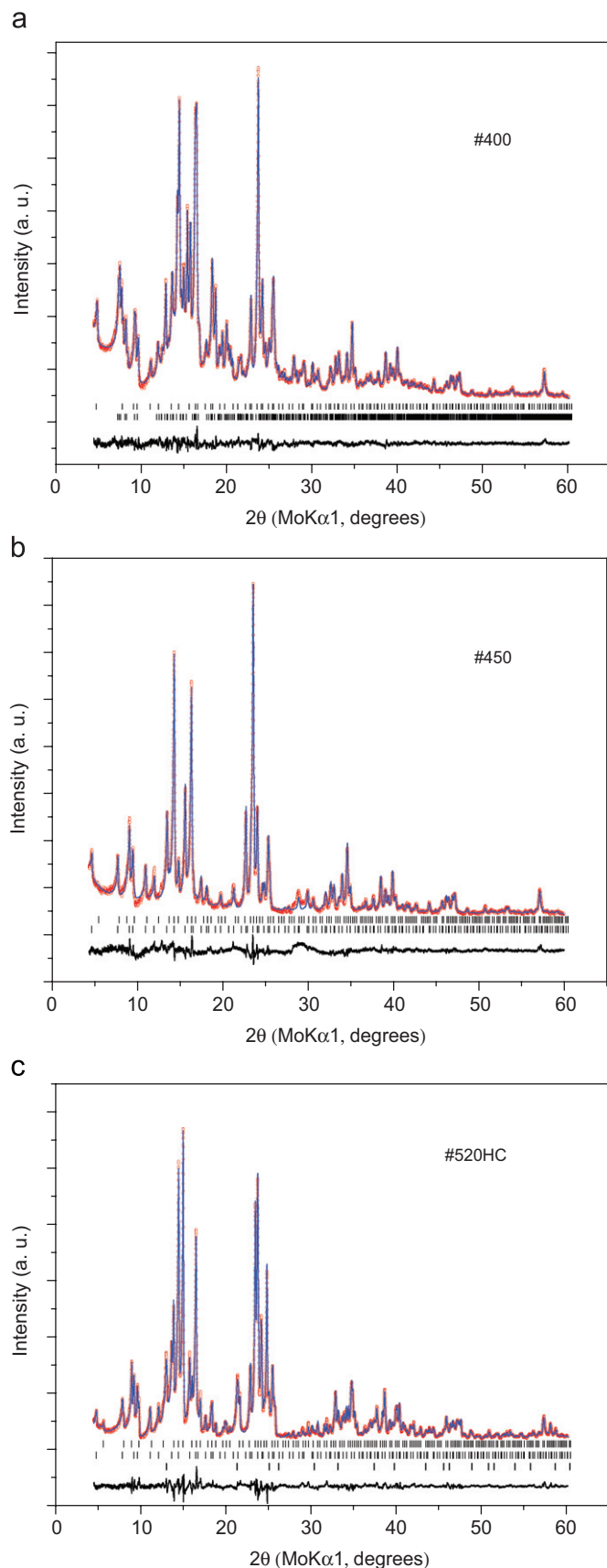
NaSi was prepared from a stoichiometric mixture of Na metal (>99.9%) and Si (99.98%). A slight excess of Na metal was mixed with silicon powder, and loaded in a Ta crucible, which was in turn sealed in a stainless steel tube using Swagelock fittings in an Ar filled glove box. The sealed tube was heated at 650 °C for three days; after the reaction, the excess Na was removed by evacuation at 300 °C for 6 h. Thermal decomposition of the ground NaSi powder sample (about 20 mg) was carried out using an h-BN (hexagonal boron nitride) cell with an inner diameter of 4 mm, and a depth of 15 mm, which was placed in a Pyrex glass tube for continuous evacuation in a furnace. Two types of h-BN cells were used, with and without a cover. The cover was also made of h-BN and had two pin through-holes with a diameter of 0.6 mm. The h-BN cell coupled with the pin-holed cover acted as the Knudsen cell. The NaSi sample loaded in the h-BN cell was heated at 340 °C under vacuum ($<10^{-4}$ Torr) in a vertical cylindrical furnace for 30 min, and the temperature was raised to the preset temperature ranging from 400 to 550 °C in 5 min. All the samples were kept at the preset temperature for a fixed interval of 90 min. The h-BN cell was pre-heated in vacuum at 1000 °C for 2 h to remove adsorbed water prior to the use. All of the sample manipulation was carried out in an Ar filled glove box.

Powder X-ray diffraction (XRD) patterns were measured using an imaging plate Guinier diffractometer (Huber 670G) with a rotating capillary goniometer and monochromated $\text{MoK}\alpha_1$ radiation ($\lambda = 0.70926$ Å). A thin Pyrex glass capillary with a diameter of about 0.3 mm was used to seal the powder sample for the XRD measurement. The powder patterns were analyzed by the Rietveld refinement program, TOPAS-Academic [28] to determine the lattice parameters and the weight fractions of the coexisting clathrates and other phases. The background due to the blank glass capillary was measured and removed from the sample profile. The imaging plate Guinier diffractometer can cover the diffraction 2θ range of 4–100° with a step of 0.005°. The diffraction pattern in a range of 4.5–60° was refined using the full profile fit with a pseudo-Voigt type profile function for each existing phase. The calibration of the imaging plate was performed using LaB_6 powder as a standard.

3. Results and discussion

NaSi was stable against heating under vacuum at temperatures below 340 °C. Above 360 °C, sodium metal vapor was evolved from NaSi, and deposited as silver mirror on the upper part of the glass tube. The samples decomposed at different temperatures {TEMP}

for 90 min without or with the pin-holed cover are referred to as #TEMP and #TEMPHC, respectively. Some typical XRD patterns obtained for #400, #450, and #520HC are shown in Fig. 2. As



can be seen from the Rietveld profile fit of the figure, the samples were mixtures of two or three phases. The Rietveld refinements were performed on all of the XRD profiles, and the results are listed in Table 1. The lattice parameters, atomic coordinates, phase fractions, temperature factors, site occupancies were all refined under the constraint that all Si sites were fully occupied, and the temperature factors of all Si atoms were the same in the same phase. In the table, only the crystallographic data of type II phase are given for comparison. The weight fractions of the constituents of the mixtures obtained at different decomposition temperatures for a fixed time of 90 min are compared in Fig. 3. In the series of the decomposition without using the cover, the sample obtained at 400 °C was a mixture of the undecomposed NaSi and the type II clathrate. At 450 °C, NaSi was almost completely converted into the type II clathrate with 7.5% contamination of type I clathrate. At 470–500 °C, the type I phase was formed with the type II, and the fraction occupied by the type I phase was about 15%. At the higher temperature of 520 °C, the fraction of the type I phase increased to more than 60%, and at 550 °C, the type I phase decomposed to crystalline Si. The type II phase was stable at 550 °C. When the mixture obtained at 520 °C was re-heated at 550 °C for 90 min in vacuum, the type I phase was decomposed to Si, keeping the fraction of the type II phase unchanged.

In the second series of a similar thermal decomposition using the pin-holed cover (#TEMPHC), the removal of Na metal was suppressed, and the vapor retained in the cell during the decomposition. At 400 °C, most of NaSi remained undecomposed; the formation of type II phase was only ~10%. At 450 °C, even though 60% of NaSi still remained undecomposed, the type I phase already appeared. At 470 °C, all of NaSi disappeared and converted to a mixture of the types I and II clathrate phases. It should be noted that the fraction of the type I phase increased with the increase in temperature. Evidently the higher decomposition temperature and the use of pin-hole cover are favorable for the formation of the type I phase, although at temperatures above 520 °C, type I phase is not stable.

The type I clathrate was prepared by decomposition of NaSi under Ar atmosphere at 410 °C [1,4]. What is the effect of the Ar atmosphere in the formation of the type I clathrate compound? Under vacuum condition, Na vapor evolved by decomposition of NaSi is rapidly removed out of the system, whereas with the presence of Ar atmosphere, Na vapor should stay for a while in the Ar atmosphere surrounding the decomposed NaSi due to the short mean-free path of Na atoms in Ar atmosphere. The existence of Na vapor in the decomposition of NaSi should be favorable for the formation of the type I clathrate compound. A similar condition can be realized by using the pin-holed cover, which can retain Na metal vapor in the h-BN cell during the decomposition. The experimental results of this study also indicate that the high decomposition temperature is favorable for the formation of the type I clathrate compound.

Note that different research groups used different decomposition temperatures for the type II clathrates: 340–420 °C by Reny et al. [4,20], 375 °C by Ramachandran et al. [5], and 425 °C by Beekman and Nolas [29]. It has been reported that varying the decomposition temperature and time results in different Na concentrations. Fig. 4 shows the decomposition temperature dependence of the lattice parameters of the two clathrate phases. The lattice parameter of the type I clathrate was constant at

Fig. 2. Rietveld refinements of the X-ray diffraction patterns of the samples: (a) #400, (b) #450, and (c) #520HC. Open circles show the observed data points and the solid line represents the calculated diffraction pattern. (a) Two-phase mixture, type II (top tick marks) and NaSi (bottom tick marks), (b) two-phase mixture, type I (top tick marks) and type II (middle tick marks), (c) three-phase mixture, type I (top tick marks), type II (middle tick marks), and Si (bottom tick marks).

Table 1

Phases found by the thermal treatment of NaSi at various temperatures; their lattice parameters, phase fractions, and atomic parameters for type II phase determined by the Rietveld refinement

#400						#400HC					
Phase	<i>a</i> (Å)	wt%	<i>R</i> factors (%)								
Type II NaSi	14.7228(2) ^a	43.5(3) 56.5(3)	<i>Rwp</i> = 2.901, <i>R</i> exp = 2.988, GOF = 0.971								
Type II	(Na _{22.56} Si ₁₃₆)										
Atom (site)	<i>X</i>	<i>y</i>	<i>z</i>	Occ	Beq (Å ²)						
Si1 (8 <i>a</i>)	1/8	1/8	1/8	1	0.78(1)						
Si2 (32 <i>e</i>)	0.21832(6)	0.21832(6)	0.21832(6)	1	0.78(1)						
Si3 (96 <i>g</i>)	0.18297(3)	0.18297(3)	0.37148(6)	1	0.78(1)						
Na1 (8 <i>b</i>)	3/8	3/8	3/8	1.01(1)	11.3(3)						
Na2 (16 <i>c</i>)	0	0	0	0.91(1)	1.92(7)						
#450						#450HC					
Phase	<i>a</i> (Å)	wt%	<i>R</i> factors (%)								
Type II	14.6855(3)	92.5(2)	<i>Rwp</i> = 5.836, <i>R</i> exp = 3.492, GOF = 1.671								
Type I	10.2028(6)	7.5(2)									
Type II	(Na _{17.12} Si ₁₃₆)										
Atom (site)	<i>x</i>	<i>y</i>	<i>z</i>	Occ	Beq (Å ²)						
Si1 (8 <i>a</i>)	1/8	1/8	1/8	1	0.95(1)						
Si2 (32 <i>e</i>)	0.21879(7)	0.21879(7)	0.21879(7)	1	0.95(1)						
Si3 (96 <i>g</i>)	0.18294(3)	0.18294(3)	0.37204(7)	1	0.95(1)						
Na1 (8 <i>b</i>)	3/8	3/8	3/8	0.96(1)	9.49(30)						
Na2 (16 <i>c</i>)	0	0	0	0.59(1)	1.00(13)						
#470						#470HC					
Phase	<i>a</i> (Å)	wt%	<i>R</i> factors (%)								
Type II	14.7003(2)	86.4(1)	<i>Rwp</i> = 4.244, <i>R</i> exp = 2.976, GOF = 1.426								
Type I	10.2068(3)	13.6(2)									
Type II	(Na _{18.72} Si ₁₃₆)										
Atom (site)	<i>x</i>	<i>y</i>	<i>z</i>	Occ	Beq (Å ²)						
Si1 (8 <i>a</i>)	1/8	1/8	1/8	1	0.68(1)						
Si2 (32 <i>e</i>)	0.21820(5)	0.21820(5)	0.21820(5)	1	0.68(1)						
Si3 (96 <i>g</i>)	0.18307(2)	0.18307(2)	0.37104(5)	1	0.68(1)						
Na1 (8 <i>b</i>)	3/8	3/8	3/8	1.04(1)	10.50(21)						
Na2 (16 <i>c</i>)	0	0	0	0.67(1)	1.65(9)						
#500						#500HC					
Phase	<i>a</i> (Å)	wt%	<i>R</i> factors (%)								
Type II	14.6555(1)	85.9(2)	<i>Rwp</i> = 4.404, <i>R</i> exp = 2.905, GOF = 1.481								
#400HC						#400HC					
Phase	<i>a</i> (Å)	wt%	<i>R</i> factors (%)								
Type II NaSi	14.7299(4) ^b	10.8(2) 89.2(2)	<i>Rwp</i> = 3.262, <i>R</i> exp = 2.165, GOF = 1.507								
Type II	(Na _{23.36} Si ₁₃₆)										
Atom (site)	<i>X</i>	<i>y</i>	<i>z</i>	Occ	Beq (Å ²)						
Si1 (8 <i>a</i>)	1/8	1/8	1/8	1	0.81(4)						
Si2 (32 <i>e</i>)	0.21869(21)	0.21869(21)	0.21869(21)	1	0.81(4)						
Si3 (96 <i>g</i>)	0.18321(9)	0.18321(9)	0.37081(22)	1	0.81(4)						
Na1 (8 <i>b</i>)	3/8	3/8	3/8	1.05(4)	15.7(11)						
Na2 (16 <i>c</i>)	0	0	0	0.96(2)	1.13(24)						
#450HC						#450HC					
Phase	<i>a</i> (Å)	wt%	<i>R</i> factors (%)								
Type II	14.7231(4)	25.2(6)	<i>Rwp</i> = 2.976, <i>R</i> exp = 2.127, GOF = 1.399								
Type I NaSi	10.2049(3) ^c	13.4(4) 61.4(7)									
Type II	(Na _{24.00} Si ₁₃₆)										
Atom (site)	<i>x</i>	<i>y</i>	<i>z</i>	Occ	Beq (Å ²)						
Si1 (8 <i>a</i>)	1/8	1/8	1/8	1	0.77(4)						
Si2 (32 <i>e</i>)	0.21601(15)	0.21601(15)	0.21601(15)	1	0.77(4)						
Si3 (96 <i>g</i>)	0.18254(7)	0.18254(7)	0.37289(18)	1	0.77(4)						
Na1 (8 <i>b</i>)	3/8	3/8	3/8	1.05(4)	12.7(9)						
Na2 (16 <i>c</i>)	0	0	0	1.07(2)	1.00(17)						
#470HC						#470HC					
Phase	<i>a</i> (Å)	wt%	<i>R</i> factors (%)								
Type II	14.7061(2)	80.9(2)	<i>Rwp</i> = 3.772, <i>R</i> exp = 2.932, GOF = 1.287								
Type I	10.2053(3)	19.1(2)									
Type II	(Na _{20.48} Si ₁₃₆)										
Atom (site)	<i>x</i>	<i>y</i>	<i>z</i>	Occ	Beq (Å ²)						
Si1 (8 <i>a</i>)	1/8	1/8	1/8	1	0.85(2)						
Si2 (32 <i>e</i>)	0.21839(8)	0.21839(8)	0.21839(8)	1	0.85(2)						
Si3 (96 <i>g</i>)	0.18294(4)	0.18294(4)	0.37119(8)	1	0.85(2)						
Na1 (8 <i>b</i>)	3/8	3/8	3/8	1.05(1)	9.78(31)						
Na2 (16 <i>c</i>)	0	0	0	0.78(13)	1.98(14)						
#500HC						#500HC					
Phase	<i>a</i> (Å)	wt%	<i>R</i> factors (%)								
Type II	14.6886(2)	52.3(2)	<i>Rwp</i> = 3.584, <i>R</i> exp = 2.652, GOF = 1.352								

Type I Si	10.2017(3) 5.4335(7)	11.2(13) 2.9(1)				Type I Si	10.2037(1) 5.4298(2)	34.6(2) 13.1(1)			
Type II	(Na _{7.20} Si ₁₃₆)					Type II	(Na _{16.00} Si ₁₃₆)				
Atom (site)	x	y	z	Occ	Beq (Å ²)	Atom (site)	x	y	z	Occ	Beq (Å ²)
Si1 (8a)	1/8	1/8	1/8	1	0.69(1)	Si1 (8a)	1/8	1/8	1/8	1	0.77(2)
Si2 (32e)	0.21759(4)	0.21759(4)	0.21759(4)	1	0.69(1)	Si2 (32e)	0.21860(7)	0.21860(7)	0.21860(7)	1	0.77(2)
Si3 (96g)	0.18307(2)	0.18307(2)	0.37089(4)	1	0.69(1)	Si3 (96g)	0.18296(4)	0.18296(4)	0.37099(7)	1	0.77(2)
Na1 (8b)	3/8	3/8	3/8	0.76(1)	9.72(24)	Na1 (8b)	3/8	3/8	3/8	0.94(1)	8.49(31)
Na2 (16c)	0	0	0	0.07(1)	1	Na2 (16c)	0	0	0	0.53(1)	0.99(15)
#520						#520HC					
Phase	a (Å)	wt%	R factors (%)			Phase	a (Å)	wt%	R factors (%)		
Type II	14.6668(3)	33.8(2)	Rwp = 3.987, R exp = 2.698, GOF = 1.478			Type II	14.6818(2)	44.0(2)	Rwp = 5.202, R exp = 3.010, GOF = 1.728		
Type I	10.2047(1)	60.7(2)				Type I	10.2052(1)	46.6(2)			
Si	5.4314(3)	5.5(1)				Si	5.4308(2)	9.4(1)			
Type II	(Na _{11.04} Si ₁₃₆)					Type II	(Na _{14.80} Si ₁₃₆)				
Atom (site)	x	y	z	Occ	Beq (Å ²)	Atom (site)	x	y	z	Occ	Beq (Å ²)
Si1 (8a)	1/8	1/8	1/8	1	1.14(4)	Si1 (8a)	1/8	1/8	1/8	1	0.98(2)
Si2 (32e)	0.21792(12)	0.21792(12)	0.21792(12)	1	1.14(4)	Si2 (32e)	0.21816(8)	0.21816(8)	0.21816(8)	1	0.98(2)
Si3 (96g)	0.18390(6)	0.18390(6)	0.37139(12)	1	1.14(4)	Si3 (96g)	0.18333(4)	0.18333(4)	0.37083(7)	1	0.98(2)
Na1 (8b)	3/8	3/8	3/8	0.98(2)	11.26(63)	Na1 (8b)	3/8	3/8	3/8	0.95(1)	9.88(37)
Na2 (16c)	0	0	0	0.20(1)	2.15(85)	Na2 (16c)	0	0	0	0.45(1)	1.54(22)
#550											
Phase	a (Å)	wt%	R factors (%)								
Type II	14.6465(5)	29.3(4)	Rwp = 5.985, R exp = 2.861, GOF = 2.091								
Si	5.4302(1)	70.7(4)									
Type II	(Na _{1.52} Si ₁₃₆)										
Atom (site)	x	y	z	Occ	Beq (Å ²)						
Si1 (8a)	1/8	1/8	1/8	1	0.97(4)						
Si2 (32e)	0.21838(16)	0.21838(16)	0.21838(16)	1	0.97(4)						
Si3 (96g)	0.18262(9)	0.18262(9)	0.37073(16)	1	0.97(4)						
Na1 (8b)	3/8	3/8	3/8	0.19(2)	7						
Na2 (16c)	0	0	0	0.00(1)	1						

GOF = Rwp/R exp.

Beq: Equivalent isotropic temperature factor.

Occ: Occupancy of site.

The Na content of type II clathrate was estimated from the occupancies of Na1 and Na2 sites.

^a a = 12.1636(4), b = 6.5481(2), c = 11.1395(4) Å, β = 118.921(2)°.

^b a = 12.1688(3), b = 6.5502(2), c = 11.1425(3), β = 118.913(2)°.

^c a = 12.1619(11), b = 6.5448(7), c = 11.1291(11), β = 118.938(7)°.

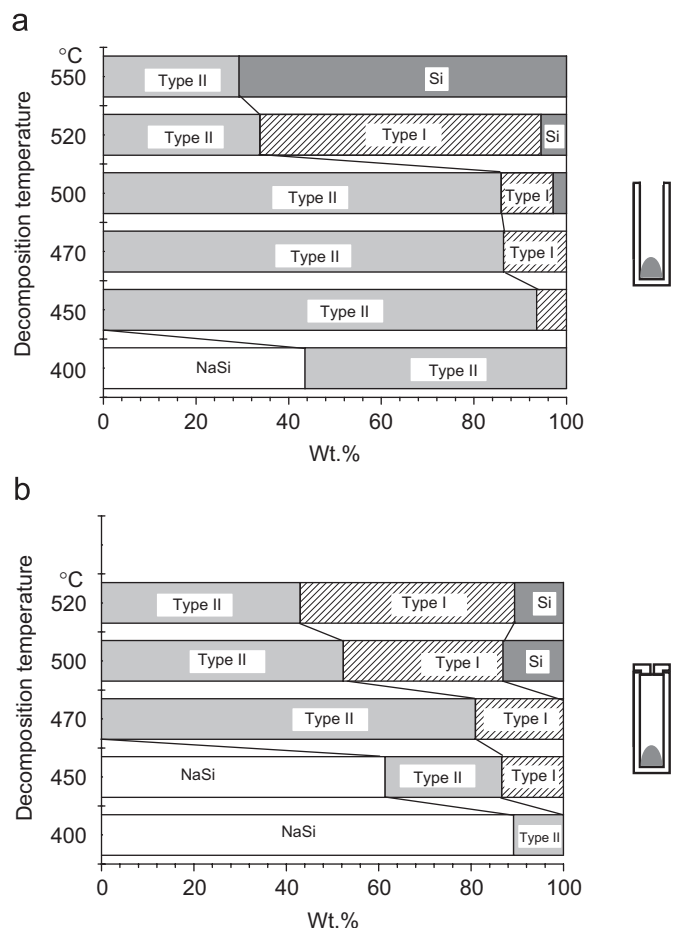


Fig. 3. Weight fraction of the clathrates and associated phases as a function of decomposition temperature: (a) without cover and (b) with the pin-holed cover.

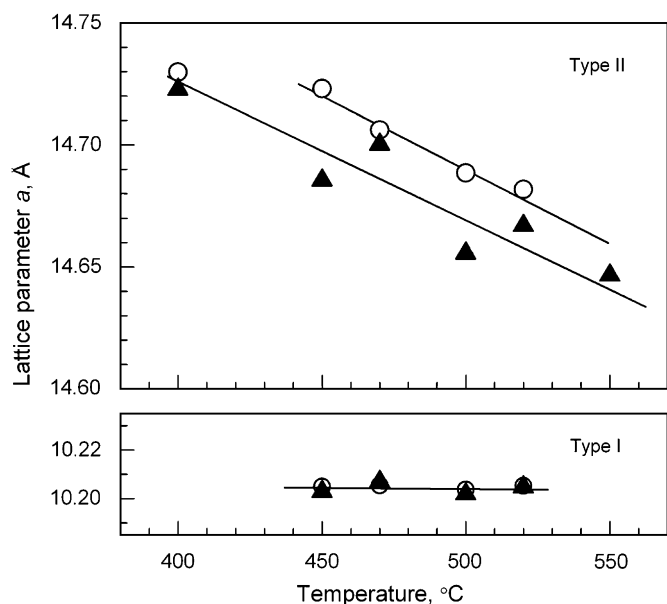


Fig. 4. Lattice parameters of the types I and II clathrate compounds as a function of the decomposition temperature using the decomposition cell without (▲) and with (○) the pin-holed cover.

$a = 10.202\text{--}10.207 \text{ \AA}$, independent of the decomposition temperature. This is due to the stoichiometry of the type I clathrate with a fixed composition of $\text{Na}_8\text{Si}_{46}$. The parameter of type I clathrate

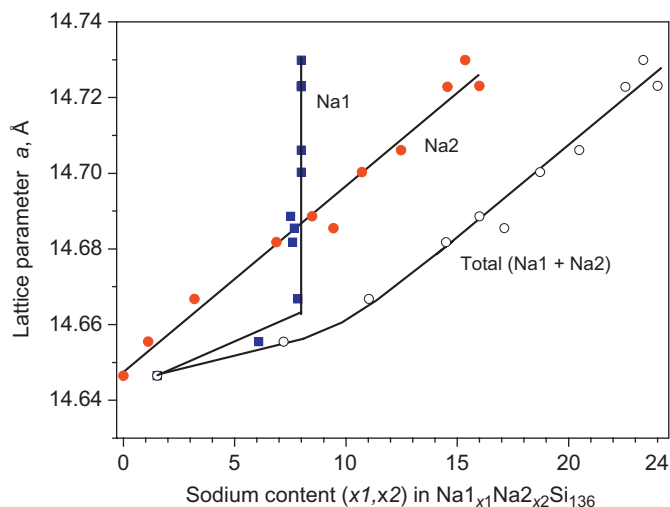


Fig. 5. Lattice parameter a against Na contents at Na1 and Na2 sites.

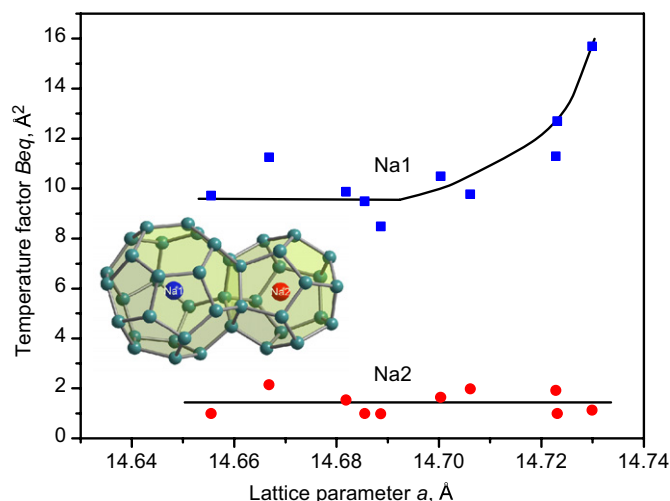


Fig. 6. Temperature factors of Na atoms at Na1 and Na2 sites against lattice parameter a of type II clathrate.

obtained in this study is in good agreement with the reported value of $10.1983(2) \text{ \AA}$ by Reny et al. [4], and $10.19648(2) \text{ \AA}$ by Ramachandran et al. [5]. The lattice parameter of the type II clathrates decreased with the increasing temperature. In Fig. 5 the lattice parameter is plotted against Na content in the Na1(8b) and Na2(16c) sites of the type II clathrates listed in Table 1. These data are in good agreement with those reported by other research groups [4,5]. The lattice parameter has a linear relationship with the Na content of the Na2 site; the Na atoms of the Na1 site were removed after the Na2 sites were almost emptied. Fig. 6 shows the equivalent isotropic temperature factors (B_{eqs}) of the Na atoms in the two different sites with varying lattice parameters. The temperature factor of the Na atom of the Na1 site in the Si hexakaidecahedral cage is about one order larger than that of the Na2 site in the Si dodecahedral cage. A similar tendency in the temperature factors of the Na atoms in the type II clathrates was pointed out by Reny et al [4] and Ramachandran et al. [5].

Taking the above data together, we would like to propose the preparation route for the two types of clathrates separately. The key point for the preparation is the decomposition temperature and the control of Na vapor pressure. In the preparation of the type II clathrate $\text{Na}_x\text{Si}_{136}$ with a minimal contamination of the

type I clathrate, excess Na metal should be first removed at temperatures below 340 °C, where no decomposition of NaSi begins, then NaSi should be decomposed at temperatures below 440 °C by prolonged heating. The staying of Na vapor should be avoided; NaSi should be shallowly loaded in a container with a sufficiently wide diameter, so that Na vapor evolved from NaSi can be removed as rapidly as possible. The lower the decomposition temperature, the longer evacuation time is required. The final concentration of Na in $\text{Na}_x\text{Si}_{136}$ varies depending on the decomposition temperature and time. A type II clathrate $\text{Na}_{1.76}\text{Na}_{2.064}\text{Si}_{136}$ with less than 1% contamination of the type I clathrate was prepared at 440 °C by evacuation for 18 h.

The type I clathrate compound $\text{Na}_8\text{Si}_{46}$ is formed at relatively high temperatures, and the presence of Na vapor is favorable. However, the type I clathrate is not thermally stable, and decomposed to crystalline Si above 520 °C in vacuum. This decomposition temperature appears to be lowered to ~500 °C in the presence of excess Na vapor as shown in Fig. 3. In an attempt to prepare the type I clathrate by evacuation, NaSi was loaded in a narrow and long glass tube (1 mm in diameter and 70 mm in depth) to keep Na vapor during the decomposition of NaSi, and heated at 450 °C under vacuum. The product obtained was found to be a mixture of 70% type I and 30% type II clathrate compounds. We have also variously changed the amount of NaSi loading, and the shape of the containers to control the Na vapor pressure during the decomposition. However, it is still difficult to obtain the phase-pure type I clathrate compound. More systematic detailed study on the Na vapor pressure suitable for the decomposition of NaSi is required.

4. Conclusions

Preparation condition for the type II clathrate compound was determined based on the thermal decomposition data of NaSi at various temperatures under vacuum. The optimal condition to prepare type II silicon clathrate $\text{Na}_x\text{Si}_{136}$ with minimal contamination with the type I phase can be proposed as the following: the starting NaSi should be thermally decomposed below 440 °C, and the rapid removal of Na vapor evolved is essentially important. The Rietveld analysis of the decomposed products at various temperatures showed that the lattice parameter of the type II clathrate was linearly decreased from 14.73 to 14.65 Å with the decrease in the Na content from 16.0 to 0 at the $\text{Na}_2(16c)$ site.

The preparation of the type I clathrate free from the type II phase was difficult. More systematic detailed study on the suitable Na vapor pressure for the NaSi decomposition is required.

Acknowledgments

This study has also been supported by a Grant-in-Aid for Scientific Research (Nos. 19105006 and 19051011) of the Ministry of Education, Culture, Sports, Science, and Technology of Japan.

References

- [1] C. Cros, M. Pouchard, P. Hagenmuller, C. R. Acad. Sci. Paris 260 (1965) 4764.
- [2] S. Kasper, P. Hagenmuller, M. Pouchard, C. Cros, Science 150 (1965) 1713.
- [3] C. Cros, M. Pouchard, P. Hagenmuller, J. Solid State Chem. 2 (1970) 570.
- [4] E. Reny, P. Gravereau, C. Cros, M. Pouchard, J. Mater. Chem. 8 (1998) 2839.
- [5] K. Ramachandran, J. Dong, J. Diefenbacher, J. Gryko, R.F. Marzke, O.F. Sankey, P.F. McMillan, J. Solid State Chem. 145 (1999) 716.
- [6] J.V. Zaikina, K.A. Kovnir, F. Haarmann, W. Schnelle, U. Burkhardt, H. Borrmann, U. Schwarz, Y. Grin, A.V. Shevelkov, Chem. Eur. J. 14 (2008) 5414.
- [7] S. Bobev, S.C. Sevov, J. Am. Chem. Soc. 123 (2001) 3389.
- [8] S. Bobev, S.C. Sevov, J. Solid State Chem. 153 (2000) 92.
- [9] M. Beekman, G.S. Nolas, J. Mater. Chem. 18 (2008) 8420851.
- [10] A. San-Miguel, P. Toulemond, High Pressure Res. 25 (2005) 159.
- [11] K.A. Kovnir, A.V. Shevelkov, Russ. Chem. Rev. 73 (2004) 923.
- [12] Ya. Murydyk, P. Rogl, C. Paul, S. Berger, E. Bauer, G. Hilscher, C. Godart, H. Noël, A. Saccone, R. Ferro, Phys. B 328 (2003) 44.
- [13] G.S. Nolas, G.A. Slack, Am. Sci. 89 (2001) 136.
- [14] S. Yamanaka, Jpn. J. Appl. Phys. 41 (2002) 5008.
- [15] G.S. Nolas, J.L. Cohn, G.A. Slack, S.B. Schujman, Appl. Phys. Lett. 73 (1998) 176.
- [16] G.S. Nolas, T.J.R. Weakley, J.L. Cohn, R. Sharma, Phys. Rev. B 61 (2000) 3845.
- [17] M.A. Avila, K. Suekuni, K. Umoe, H. Fukuoka, S. Yamanaka, T. Takabatake, Appl. Phys. Lett. 92 (2008) 041901.
- [18] H. Kawaji, H. Horie, S. Yamanaka, M. Ishikawa, Phys. Rev. Lett. 74 (1995) 1427.
- [19] S. Yamanaka, E. Enishi, H. Fukuoka, M. Yasukawa, Inorg. Chem. 39 (2000) 56.
- [20] A. Ammar, C. Cros, M. Pouchard, N. Jaussaud, J.-M. Bassat, G. Villeneuve, M. Duttine, M. Ménétrier, E. Reny, Solid State Sci. 6 (2004) 393.
- [21] S. Saito, A. Oshiyama, Phys. Rev. B 51 (1995) 1628.
- [22] K. Moriguchi, M. Yonemura, S. Munetoh, S. Shibagaki, A. Shintani, S. Yamanaka, Phys. Rev. B 61 (2000) 9859.
- [23] M. Guloy, R. Ramlau, Z. Tang, W. Schnelle, M. Baitinger, Y. Grin, Nature 443 (2006) 320.
- [24] K. Moriguchi, S. Munetoh, A. Shintani, Phys. Rev. B 62 (2000) 7138.
- [25] M. Pouchard, C. Cros, P. Hagenmuller, E. Reny, A. Ammar, M. Ménétrier, J.-M. Bassat, Solid State Sci. 4 (2002) 723.
- [26] S. Yamanaka, H. Horie, H. Nakano, M. Ishikawa, Fullerene Sci. Tech. 3 (1995) 21.
- [27] J. Gryko, R.F. Marzke, A. Lamberton Jr., T.M. Tritt, M. Beekman, G.S. Nolas, Phys. Rev. B 71 (2005) 115208.
- [28] A. Coelho, TOPAS-Academic v 4.1: General Profile and Structure Analysis Software for Powder Diffraction Data, Brisbane, 2007.
- [29] M. Beekman, G.S. Nolas, Phys. B 383 (2006) 111.